Acta Cryst. (1964). **17**, 817

Stacking Fault Probabilities in Hexagonal Cobalt

By G. B. Mitra and N. C. Halder

Department of Physics, Indian Institute of Technology, Kharagpur, India

(*Received* 17 *November* 1962 *and in revised form* 1 *July* 1963)

The effect of cold working and annealing on the stacking fault probabilities in h.c.p. cobalt has been studied. The composite broadening has been attributed to three causes — particle size, lattice strain and stacking faults. The particle-size and strain broadening have been separated in each case. The assumed strain models were both of Gaussian and Cauchy types. Line breadth measurements have been also carried out. Fault parameters decreased with annealing but there was no evidence of complete annihilation.

Introduction

Anomalous line broadening in hexagonal close-packed cobalt was first noticed by Van Arkel (1939) who explained it in terms of impurity content, but broadening due to a fault which breaks the regular sequence of close packed atomic layers has been studied by Edwards & Lipson (1942). Their main finding was that the broadening of lines from hexagonal cobalt differs for different reflexions in a way which cannot be explained solely on the basis of particle size or strain; considerations of growth faulting and the assumption of its regular occurrence could explain the apparent discrepancies in line broadening. Wilson (1942) developed a theory which considered the random distribution of faults, and showed that in h.c.p. cobalt the reflexions with l even were broadened more than those with l odd and that there was not much change in the total intensity of the reflexions. Wilson's theory also provided for calculations of the probability of faulting. The frequency of faults in Edwards & Lipson's (1942) specimen was calculated on this theory and it was found that on the average there occurred about one faulty plane in every ten. The first systematic investigation of faulting in h.c.p. cobalt was carried out by Anantharaman & Christian (1956). They performed a line shape analysis, confining their attention to the {101} line. They observed that in addition to the growth faults deformation faults also occurred in the sample. The spontaneously transformed cobalt sample studied by them contained growth faults predominantly, whereas deformed cobalt after complete martensitic transformation showed mainly deformation faulting. Further investigations were carried out by Houska & Averbach (1958) and Houska, Averbach & Cohen (1960). These workers have studied the correlation between phase change principle and stacking fault density.

In spite of all these advances, there remained many more questions to consider, for instance — distribution of either of the faults, the effect of temperature of annealing on the faults, the amount of broadening due to small domain size and lattice strain in the fault-broadened reflexions, the influence of elastic anisotropy on the distribution of strain and stress. The present investigation is an attempt to elucidate some of these. None of the previous investigators has attributed the line broadening to all three possible causes; they have neglected the effect of domain size and lattice strain. This omission is partly justified in the transformed specimens but it is not necessarily correct in every case. Also the strain distribution function considered earlier was only of the Cauchy type. Keeping all these points in view, it has been decided here to apply the recently developed theories, referring to the three possible causes, to the study of particle size, lattice strain and stacking faults in faulted h.c.p. cobalt.

Review of theories of fault probability in the h.c.p. structure

Wilson (1942) developed a theory for calculating fault probability in h.c.p. crystals. He showed that only reflexions affected by stacking faults have $h-k=3t\pm1$ with all values of l except zero. This theory, however, is only applicable to crystals having growth faults. Christian (1954) has suggested an independent method of calculating deformation fault probability in h.c.p. crystals. He showed that the integral breadths of the lines in an h.c.p. crystal with deformation faulting are identical with those in a similarly faulted f.c.c. crystal (Patterson, 1952). Gevers (1954) has treated a more general case which has been later extended by Anantharaman & Christian (1956). Warren (1959) has suggested a method which is more useful and systematic. He has used the full width at half maximum intensity and derived the expressions

for l even

$$B_{\frac{1}{2}}(2\theta) = (360/\pi^2)\tan\theta|l|(d/c)^2(3\alpha+3\beta), \qquad (1)$$

for l odd

$$B_{\frac{1}{2}}(2\theta) = (360/\pi^2)\tan\theta|l|(d/c)^2(3\alpha+\beta), \qquad (2)$$

where d is the interplanar spacing of the reflecting

plane, $c = 2d_{002}$, $B_{\frac{1}{2}}(2\theta)$ the width at half maximum intensity expressed in degrees, α the deformation fault probability and β the growth fault probability.

In the theories which have been discussed above, only the line breadths are measured from which fault probabilities are calculated. Houska & Averbach (1958) have developed a method of line shape analysis for h.c.p. crystals. They showed that the diffracted power per unit arc length is

$$P'_{2\theta} = K'\Sigma A_n^P A_n^{SF} A_n^D \exp 2\pi i n h'_3 \qquad (3)$$

where

the particle size coefficients

$$A_n^P = N_n/N, \qquad (4)$$

the distortion coefficients

$$A_n^D = \langle \exp (x_n h + y_n k + z_n l) \rangle, \qquad (5)$$

the stacking fault coefficients

$$A_n^{SF} = (\tfrac{3}{2}P_n^0 - \tfrac{1}{2}) + i\sqrt{3}/2\,(P_n^+ - P_n^-) \qquad (6)$$

in which P_n^0, P_n^+ and P_n^- represent the probabilities for finding the relative translations (0, 0, 0), $(\frac{2}{3}, \frac{1}{3}, 0)$ and $(-\frac{2}{3}, -\frac{1}{3}, 0)$, respectively, at a separation of n layers and K' is a constant not affecting the peak shape with h'_3 the corresponding orthorhombic indices. From this theory it is seen that $A^{SF} = 1{\cdot}00$ for $h-k = 3t$ (t being an integer,) and accounts for fault broadening only for reflexions of the type $h-k = 3t \pm 1$. From a plot of logarithmic stacking fault coefficients *versus* n one can estimate α and β. Probably the approach of Warren (1959) is easier and his theory can be applied to particle size and strain separately. The power distribution per unit length is now described by

$$P'_{2\theta} = K'\Sigma A_n^S A_n^D \cos 2\pi n (h'_3 - l') \qquad (7)$$

in which $(h'_3 - l') = 2|\mathbf{a}_3|(\sin\theta - \sin\theta_0)/\lambda$ where $|\mathbf{a}_3|$ is a fictitious distance chosen to correspond to the $\sin\theta$ interval within which the peak is expressed as a Fourier series. The coefficients A_n^S include the effect of both domain size and faultings. Then from the initial slopes of the graphs A_n^S against L, where L is a measure of distance and is obtained from Warren's (1959) formula, it can be shown that

for $h-k = 3t \pm 1$ and l even

$$-(dA_L^S/dL)_0 = 1/D + (|l|d/c^2)(3\alpha + 3\beta), \qquad (8{\cdot}1)$$

for $h-k = 3t \pm 1$ and l odd

$$-(dA_L^S/dL)_0 = 1/D + (|l|d/c^2)(3\alpha + \beta), \qquad (8{\cdot}2)$$

and for $h-k = 3t$

$$-(dA_L^S/dL)_0 = 1/D, \qquad (8{\cdot}3)$$

where D is the average particle size. If one assumes $1/D$ to be negligibly small or constant for several planes, estimation of α and β becomes simpler.

Derivation of an expression for integral width of the faulted reflexion

For a faulted hexagonal crystal the peak shape is described (Warren, 1959) by

$$Y = \sum_{m=-\infty}^{+\infty} x^{|m|} \cos \pi m (h_3 - l) = \frac{1-x^2}{1+x^2-2x\cos\pi(h_3-l)} \qquad (9)$$

where

$$x = 1 - (3\alpha + 3\beta)/2 \text{ for } l \text{ even} \qquad (10{\cdot}1)$$

and

$$x = 1 - (3\alpha + \beta)/2 \text{ for } l \text{ odd.} \qquad (10{\cdot}2)$$

Now it can be seen that Y is maximum at $(h_3 - l) = 0$ and minimum at $(h_3 - l) = \pm\frac{1}{2}$.

Therefore $$Y_{\max} = (1+x)/(1-x). \qquad (11)$$

The integral width can be written

$$B_i(h_3) = \frac{\int_{-\frac{1}{2}}^{+\frac{1}{2}} Y d(h_3 - l)}{Y_{\max}} \qquad (12)$$

or

$$B_i(h_3) = \frac{4(1-x)}{\pi(1+x)} \tan^{-1}\left(\frac{1+x}{1-x}\right). \qquad (13)$$

Since the quantity $x \simeq 1$ the above expression to a good approximation becomes

$$B_i(h_3) = (1-x). \qquad (14)$$

This can be compared with Warren's expression

$$B_{\frac{1}{2}}(h_3) = 2/\pi\,(1-x) \qquad (15)$$

where the width at half maximum intensity has been used. On the powder pattern if $B_i(2\theta)$ be the integral width expressed in degrees then from a relation (Fig. 1)

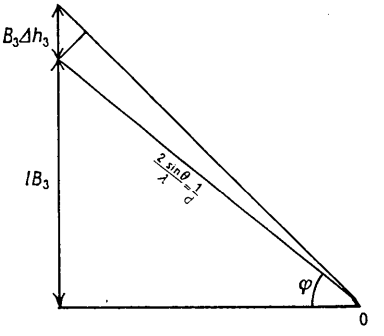

Fig. 1. Relation between the diffraction vector and the hexagonal axes.

between the diffraction vector and the hexagonal axes it can be seen that

$$B_i(2\theta) = \frac{180\lambda|\mathbf{B}_3|\sin\varphi B_i(h_3)}{\pi\cos\theta} \qquad (16{\cdot}1)$$

where

$$1/|\mathbf{B}_3| = c = 2d_{002} \qquad (16{\cdot}2)$$

and

$$|\sin\varphi| = |l|\,|\mathbf{B}_3|\,d\,. \qquad (16\cdot3)$$

Combining equations (14) and (16) we now obtain for l even

$$B_i(2\theta) = (180/\pi)\tan\theta\,|l|\,(d/c)^2(3\alpha+3\beta) \qquad (17\cdot1)$$

and for l odd

$$B_i(2\theta) = 180/\pi\tan\theta\,|l|\,(d/c)^2(3\alpha+\beta). \qquad (17\cdot2)$$

Sample preparation and X-ray diffraction procedure

Cobalt rods supplied by Johnson, Matthey and Co., Ltd., London, have been used for the present investigation. Spectroscopic analysis showed traces of iron and nickel. All measurements were conducted with fine grained powder filed from cobalt rods. Powder was prepared from the rods by grinding with an alundum wheel and then magnetically separated. The samples were passed through a sieve having 300 meshes per square inch and then subjected to heat treatment in an electric vacuum furnace. The input voltage was stabilized and controlled. The samples were put in quartz tubes with one end sealed and heated slowly. Six samples were heated for twenty-four hours at temperatures of 100, 200, 300, 410, 500 and 600 °C respectively. The cooling was controlled in the furnace itself and kept very slow so that it reached room temperature after about twenty-four hours. A difference of temperature of the order of ±2 °C was easily detected with a chromel–alumel thermocouple. The annealed samples needed pulverizing to enhance h.c.p. formation. With an agate mortar and pestle this process took about 150 to 200 blows and thereby checked (Anantharaman, 1960) f.c.c. phase transformation at room temperature.

Thin cylinders about 0·5 mm in diameter were rolled on clean glass plates after mixing the cold worked and annealed powder with a dilute solution of collodion in amyl acetate. Throughout the work a Norelco diffraction unit, and cobalt radiation filtered through an iron filter and monochromatized by a bent quartz crystal monochromator, were used. The photographs were taken in a Unicam 9 cm vacuum powder camera. The intensity distributions in the powder lines were first determined with the help of a Withol chart recording microphotometer and then repeated with a Hilger non-recording microphotometer. With the latter instrument the readings were taken every quarter rotation of the micrometer screw. By comparing the two sets of microphotometer plots, it was possible to construct the intensity profile of individual diffraction lines. Finally, the tails of all the diffraction profiles were carefully recovered from the background level of the microphotometer tracing by the method of envelopes. Details of this experimental technique have already been described by Halder (1963).

Fourier analysis of the line shapes

All the line profiles were corrected for instrumental broadening with the profiles of the fully annealed sample at 600 °C. The nearest fault-free lines were chosen for the correction of stacking-fault broadened reflexions 101, 102 and 103. The Fourier coefficients were determined by Stokes's (1948) method and plotted against L, where L is calculated from $L=n|a_3|$ and $|a_3|$ from

$$\frac{2\,|a_3|\,(\sin\theta-\sin\theta_0)}{\lambda} = \pm\tfrac{1}{2}\,,$$

θ and θ_0 corresponding to the Bragg angles for which the height of the intensity profile is maximum and minimum. The particle size and strain for these reflexions are considered to be the same as those for 100, 110, 200, 002 and 004. Though hexagonal cobalt is anisotropic, this approximation is justified. Halder (1963) has shown that the anisotropy factor in the case of deformed and annealed cobalt is not very large, the mean deviation from mean strain being about 6%.

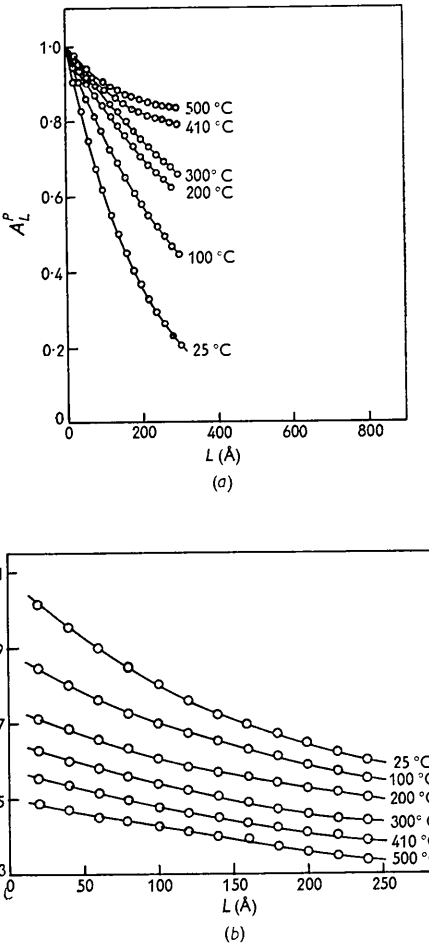

Fig. 2. (*a*) Plot of the particle size coefficients *versus* distance for cold worked h.c.p. cobalt. (*b*) Plot of the r.m.s. strain *versus* distance for cold worked h.c.p. cobalt. Both (*a*) and (*b*) obtained after assuming Gaussian distribution of strain.

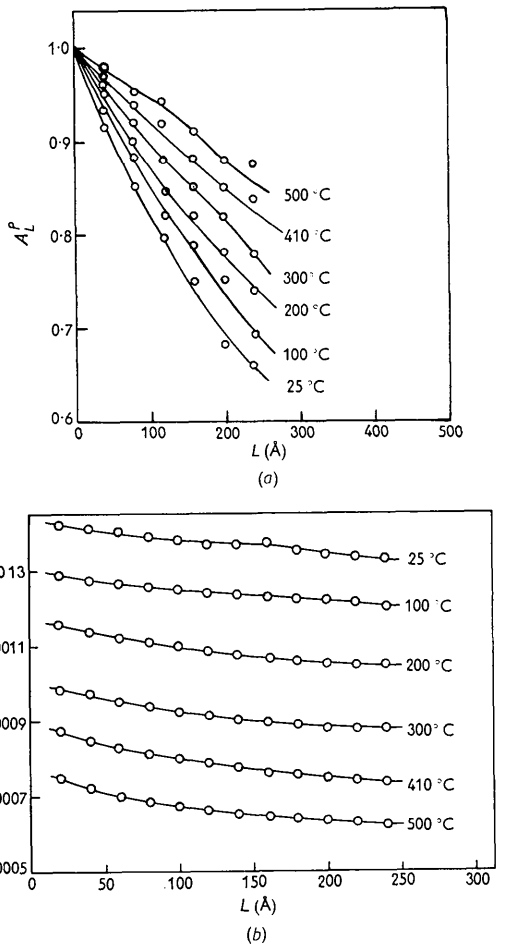

Fig. 3. (*a*) Plot of the particle size coefficients *versus* distance for cold worked h.c.p. cobalt. (*b*) Plot of the root mean square strain *versus* distance for cold worked h.c.p. cobalt. Both (*a*) and (*b*) obtained after assuming Cauchy distribution of strain.

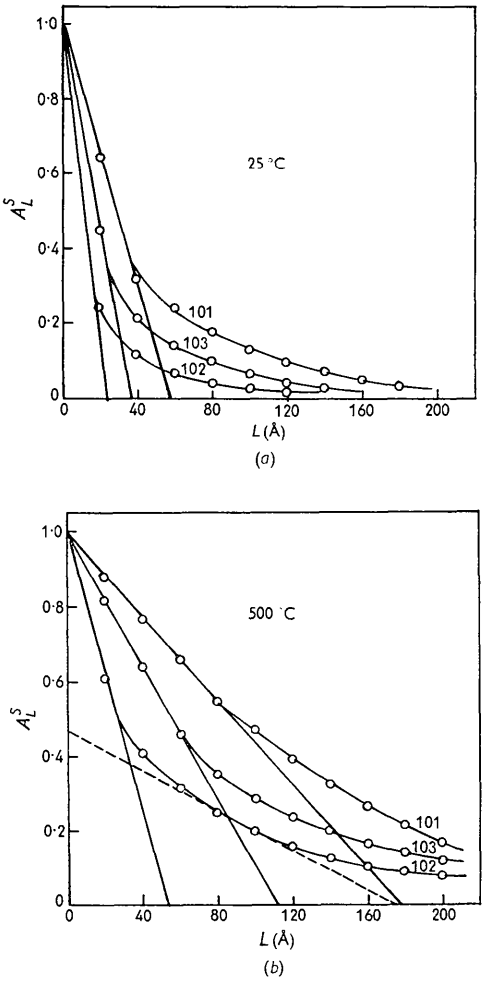

Fig. 4. Plot of the stacking fault coefficients *versus* distance for (*a*) cold worked and (*b*) annealed (at 500 °C) h.c.p. cobalt. Plots for other annealed samples are similar and consequently not shown here.

and that from mean particle size being negligibly small. Besides, there is no other suitable reflexion which can be used to find the particle size and strain only in $10l$ directions for which faultings are being studied. To avoid this difficulty to a good approximation the 'average' values of the particle size and strain of the fault-unaffected reflexions 100, 110, 200, 002 and 004 have been taken. For a hexagonal crystal the distortion coefficients are given (Warren, 1959) by

$$A_L^D = \exp\left(-\frac{2\pi^2 L^2}{d^2}\langle\varepsilon_L^2\rangle\right)$$

for Gaussian distribution of strain and

$$A_L^D = \exp\left(-\frac{\pi^2 L}{Cd}\langle\varepsilon_L^2\rangle\right)$$

for Cauchy distribution of strain, where d is the interplanar spacing of the reflexion, C the cut-off point (after Williamson & Smallman, 1954) and $\langle\varepsilon_L^2\rangle$ the mean-square strain averaged over a distance L.

Graphs were plotted for lnA_L against $1/d^2$ and lnA_L against $1/d$ for different values of L. The intercepts gave directly the coefficients of particle size and the slopes the strain. The particle size and strain plots are shown in Figs. 2 and 3. The strain values thus obtained have been utilized to correct the coefficients of fault-broadened reflexions for distortion broadening. The plots of coefficients against L are shown in Fig. 4(*a*), (*b*), the former for the cold worked sample and the latter for that annealed at 500 °C. Then the equations (8) gave α and β directly when the average value of D was substituted. These values are given in Table 4, where the difference between the two sets shows the effect of annealing on recovering of the stacking faults.

Strain and particle size corrections in the line breadth measurements

The line breadth measurements have been also made after recovering the pure diffraction profiles. The particle-size and strain broadening for these reflexions were corrected from the broadening of the fault-free reflexions as follows.

Let us consider that the total line breadth of the faulted reflexions 101, 102 and 103 be written as

$$B_i = (K_1/\cos\theta) + K_2 \tan\theta + B_i^F \qquad (18)$$

where B_i is the integral width when all the effects are present. The first and the second term of the right hand side take account of the particle-size and strain broadening respectively. The constants K_1 and K_2 can be determined from 100, 110, 200, 002 and 004 reflexions. Halder & Mitra (1963) have separated the particle size and strain broadening for these reflexions where it has been shown that there is slight anisotropy in these two quantities. With the same arguments as in the previous section and also following Rao & Anantharaman (1962), if the anisotropy factor is neglected, it is possible to know K_1 and K_2. Actually $K_1 = \lambda/D$ and $K_2 = 2\varepsilon$ where λ is the wave length of the radiation used, D the mean particle size and ε the mean strain. Thus evaluated K_1 and K_2 are shown in Table 1.

With these values when the first two terms are computed the results shown in Table 2 are obtained.

Expressing B_i^F in degrees and using equations (17) another set of α and β has been calculated. This is shown in Table 4,

Results and discussion

The particle size and strain obtained from line shape analysis are shown in Table 3. The fault probabilities measured from three different considerations are also illustrated in Table 4.

The reflexions of type $h-k=3t$ (t being an integer) are much sharper than those of type $h-k=3t\pm1 (l\neq 0)$. This is because in the former type the broadening is due to particle size and lattice strain whereas in the latter type an extra broadening due to faulting has been added. In this investigation the intensity distribution in the diffraction lines has been analysed by two different methods, *viz*, (*a*) line shape analysis by the method of Warren (1959) and (*b*) line breadth measurement by the method due to Hall (1949) .The domain size obtained by line shape analysis is quite small (250∼1800 Å) and so is the strain (0·0015∼0·0005). But the line breadth measurements show comparatively higher particle sizes (1000∼6000 Å) and greater

Table 1. *Value of the constants K_1 and K_2*

Temperature	K_1 (10^{-3})	K_2 (10^{-3})
25 °C	1·58	11·10
100	1·21	9·30
200	0·88	6·80
300	0·72	4·70
410	0·50	3·10
500	0·30	2·00

Table 2. *Corrected integral widths of* 101 *and* 102 *and* 103 *reflexions*

	B_i^F (10^{-3}) (radians)		
Temp. (°C)	101	102	103
25	20·56	55·93	46·44
100	16·38	42·00	37·00
200	13·22	33·60	29·85
300	10·39	29·38	23·46
410	8·55	26·37	19·31
500	7·17	23·56	16·18

Table 3. *Particle size and lattice strain determined from line shape analysis and line breadth measurement*

	Line shape analysis				Line breadth measurement	
	Gaussian strain		Cauchy strain			
Temperature	D	$\langle\varepsilon^2\rangle_{L=0}^{1\|2}$	D	$\langle\varepsilon^2\rangle_{L=0}^{1\|2}$	D	$\langle\varepsilon\rangle$
25 °C	246 Å	0·00108	633 Å	0·00145	1125 Å	0·00555
100	430	0·00090	780	0·00132	1480	0·00465
200	680	0·00076	900	0·00120	2020	0·00340
300	830	0·00065	1150	0·00102	2415	0·00235
410	1000	0·00057	1400	0·00093	3340	0·00155
500	1120	0·00052	1760	0·00081	5970	0·00100

Table 4. *Fault probabilities from line shape analysis and line breadth measurement*

	Line shape analysis				Line breadth measurements	
	Gaussian		Cauchy			
Temperature	α_1	β_1	α_2	β_2	α_3	β_3
25 °C	0·021	0·051	0·029	0·047	0·009	0·014
100	0·018	0·040	0·023	0·034	0·008	0·010
200	0·012	0·036	0·015	0·034	0·007	0·007
300	0·008	0·034	0·009	0·034	0·005	0·008
410	0·006	0·032	0·007	0·029	0·003	0·008
500	0·004	0·030	0·007	0·022	0·003	0·007

strains (0·0055~0·0010). It therefore appears that though the magnitudes of domain sizes and strain are different in these two analyses, their relative contribution to the total broadening is more or less the same.

Michell & Haig (1957) have investigated deformed nickel filings and found that the particle sizes obtained by line shape analysis are smaller than those obtained by line breadth measurements. The divergencies are due to the different quantities they measure. While the line shape analysis measures the average thickness of the coherently diffracting columms of layers in the *hkl* direction the line breath analysis measures the cube root of the average particle volume. Also we have not considered the particle size distribution function which affects the tails of line profiles. This means that some amount of uncertainty is always introduced in the line shape analysis. These two reasons perhaps explain the different values of the two measurements.

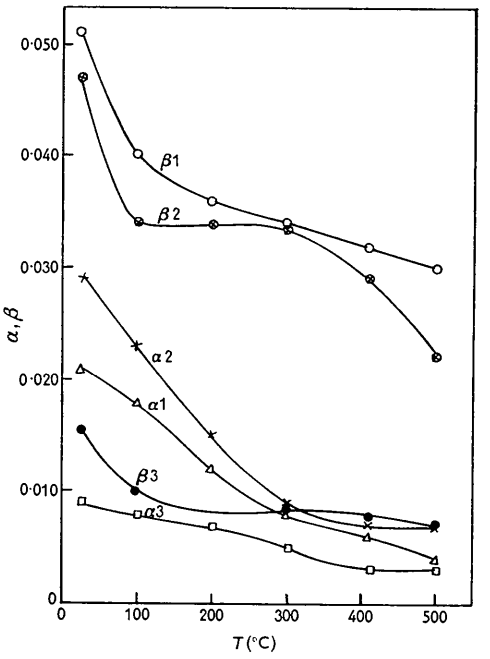

Fig. 5. Plot of the deformation (α) and growth (β) fault probabilities *versus* temperature for cold worked and annealed h.c.p. cobalt.

The plots of deformation and growth fault probabilities are shown in Fig. 5. Both of them decrease with the grain growth. α decreases at a faster rate than β. Houska, Averbach & Cohen (1960) obtained results in agreement for α but have not reported any definite trend for β. This is probably due to the effects of particle size and lattice strain which they considered to be insignificant in course of their investigation. It is also obvious from Fig. 5 that the annealing out of a deformation fault may be possible whereas the growth fault continues to exist. This is also in accordance with the sharpening effect of the reflexions; *i.e.* the reflexions with l odd become relatively sharper than those with l even with annealing. A possible explanation has been suggested by Houska, Averbach & Cohen (1960). The unstable f.c.c. phase which has been formed during the annealing process and comprises mainly deformation faults is restored to the stable h.c.p. phase during the cooling process and hence the deformation faulting decreases.

It is also observed that the faults are not equally distributed, β being always greater than α. Mitra (1963) has recently shown that for deformed and annealed metals, the strain distribution is neither Gaussian nor of the Cauchy type, but lies between these two extremes. Assuming this result to hold good also for cobalt, the strain distribution can be taken to be approximately the mean of the two extreme cases. Hence the average values of α and β are taken for the considerations which follow. At about 500 °C $\beta=0{\cdot}026$ and $\alpha=0{\cdot}006$. Now if, as suggested by Houska & Averbach (1958), the line {102} in Fig. 4(*b*) can be considered as consisting of two linear parts as shown by the dashed line in the figure, the slope of the dashed line gives $\alpha=0{\cdot}004$ and β negligibly small. This shows that at this temperature some martensitic transformation (Houska & Averbach, 1958) has taken place with the formation of two out of phase h.c.p. cobalt. We have considered only the {102} line because experimentally this line appeared to be superposition of one broad and one sharp line (Edwards & Lipson, 1942; Houska & Averbach, 1958).

References

Anantharaman, T. R. (1960). *Trans. Indian Inst. Met.* **13**, 374.

Anantharaman, T. R. & Christian, J. W. (1956). *Acta Cryst.* **9**, 479.

Christian, J. W. (1954). *Acta Cryst.* **7**, 415.

Edwards, O. S. & Lipson, H. (1942). *Proc. Roy. Soc.* A. **180**, 268.

Gevers, R. (1954). *Acta Cryst.* **7**, 337.

Halder, N. C. (1963). *Phil. Mag.* **8**, 273.

Halder, N. C. & Mitra, G. B. (1963). *Phil. Mag.* **8**, 1985.

Hall, W. H. (1949). *Proc. Phys. Soc., Lond.* **62**, 741.

Houska, C. R. & Averbach, B. L. (1958). *Acta Cryst.* **11**, 139.

Houska, C. R., Averbach, B. L. & Cohen, M. (1960). *Acta Metallurg.* **8**, 81.

Michell, D. & Haig, F. D. (1957). *Phil. Mag.* **2**, 15.

Mitra, G. B. (1963). *Acta Cryst.* **16**, 429.

Paterson, M. S. (1952). *J. Appl. Phys.* **23**, 805.

Rao, P. R. & Anantharaman, T. R. (1962). *Phil. Mag.* **7**, 705.

Stokes, A. R. (1948). *Proc. Phys. Soc. Lond.* **61**, 381.

Van Arkel, A. E. (1939). *Reine Metalle.* p. 330. Berlin: Springer.

Warren, B. E. (1959). *Progr. Met. Phys.* **8**, 147.

Williamson, G. K. & Smallman, R. E. (1954). *Acta Cryst.* **7**, 574.

Wilson, A. J. C. (1942). *Proc. Roy. Soc.* A, **180**, 277.